

Stoichiometric Photoisomerization of Mononuclear Ruthenium(II) Monoaquo Complexes Controlling Redox Properties and Water Oxidation Catalysis

Hirosato Yamazaki,[†] Tomoya Hakamata,[†] Manabu Komi,[†] and Masayuki Yagi^{*,†,‡}

[†]Department of Materials Science and Technology, Faculty of Engineering, and Center for Transdisciplinary Research, Niigata University, 8050 Ikarashi-2, Niigata 950-2181, Japan

[‡]Precursory Research for Embryonic Science (PRESTO), Japan Science and Technology Agency (JST), 4-1-8 Honcho, Kawaguchi, Saitama 332-0012, Japan

S Supporting Information

ABSTRACT: Although various reactions involved in photoexcited states of polypyridyl ruthenium(II) complexes have been extensively studied, photoisomerization of the complexes is very rare. We report the first illustration of stoichiometric photoisomerization of *trans*-[Ru(tpy)(pynp)OH₂]²⁺ (**1a**) [tpy = 2,2':6',2''-terpyridine; pynp = 2-(2-pyridyl)-1,8-naphthyridine] to *cis*-[Ru(tpy)(pynp)OH₂]²⁺ (**1a'**) and the isolation of **1a** and **1a'** for X-ray crystallographic analysis. Polypyridyl ruthenium(II) aquo complexes are attracting much attention related to proton-coupled electron transfer and water oxidation catalysis. We demonstrate that the photoisomerization significantly controls the redox reactions and water oxidation catalyses involving the ruthenium(II) aquo complexes **1a** and **1a'**.

Ruthenium(II) complexes with polypyridyl ligands have been extensively studied because they exhibit a diverse variety of excited-state phenomena, including photoluminescence, photoredox chemistry, photosubstitution and photoisomerization processes.^{1–7} The luminescent excited state is usually a triplet metal-to-ligand charge transfer (³MLCT) state. In some cases, thermal excitation of ³MLCT is known to allow a triplet ligand field (³d–d) excited state, and the latter state is assumed to be involved in a dissociative mechanism for photosubstitution.^{8–10} As far as we know, there has been only one report on photoisomerization of polypyridyl ruthenium(II) aquo complexes: Meyer and co-workers¹⁰ studied the photoisomerization of *cis*-[Ru(bpy)₂(OH₂)₂]²⁺ (bpy = 2,2'-bipyridine) to the *trans* form in water. In this case, the *trans* form was present as a photostationary state and slowly reverted to the original *cis* form. On the other hand, polypyridyl ruthenium(II) aquo complexes have also been intensively studied because of the unique proton-coupled electron-transfer reactions¹¹ and oxidative catalyses^{12–14} by the complexes. On the basis of comprehensive studies using a diverse variety of ruthenium(II) aquo complexes, Meyer suggested that the proton-coupled redox reactions depend on the σ -donating and π -accepting abilities of the five ancillary ligands for ruthenium aquo complexes.¹⁵ Recently, several ruthenium(II) aquo complexes have been reported to act as water oxidation catalysts.^{16–23}

trans-[Ru(tpy)(pynp)Cl]⁺ (**1**) (tpy = 2,2':6',2''-terpyridine; pynp = 2-(2-pyridyl)-1,8-naphthyridine) was synthesized as an

active catalyst for water oxidation.²⁴ However, the corresponding aquo complex has been difficult to isolate with high purity. In the present work, we found that *trans*-[Ru(tpy)(pynp)OH₂]²⁺ (**1a**) is stoichiometrically photoisomerized to *cis*-[Ru(tpy)(pynp)OH₂]²⁺ (**1a'**). The photoisomerization enables either **1a** or **1a'** to be isolated in high yield and purity. We report here the X-ray crystallographic structures of **1a** and **1a'** as well as the results of our studies of their redox reactions and water oxidation catalyses, both of which are significantly controlled by the photoisomerization.

1 was synthesized by the reductive ligand exchange reaction of Ru(tpy)Cl₃ with pynp and characterized by electrospray ionization mass spectrometry, NMR spectroscopy, and X-ray crystallographic analysis. Two-dimensional (2D) NMR spectra of **1** indicated that **1** is stable and remains in the *trans* configuration in acetone-*d*₆ (Figure S1 in the Supporting Information). ¹H NMR analysis of **1** in water showed that **1** is stoichiometrically converted to **1a** over 24 h by exchange of the Cl[−] ligand with solvent water (Figure S2). The *trans* configuration of **1a** in water was also corroborated by 2D NMR data (Figure S3). Addition of NH₄PF₆ to the aqueous solution of **1a** gave crystals of **1a**(PF₆)₂, which was characterized by X-ray crystallographic analysis (Table S1 in the Supporting Information; see below).

When the aqueous solution of **1a** was irradiated with visible light ($\lambda > 420$ nm, 180 mW cm^{−2}), the peak at 9.6 ppm in the ¹H NMR spectrum assigned to **1a** decreased with increasing irradiation time and disappeared completely after 25 min under the conditions employed. Alternatively, a new peak at 8.9 ppm increased correspondingly with the decrease in the 9.6 ppm peak (Figure S4). The 2D NMR data after completion of the photochemical reaction corroborated formation of the *cis* form **1a'** (Figure S5). Crystals of **1a'** were isolated by addition of NH₄PF₆ and characterized by X-ray crystallographic analysis (Table S2; see below). These results showed that **1a** is stoichiometrically photoisomerized to **1a'** in water by visible light (Scheme 1). The internal quantum yield for the photoisomerization was shown to be 1.5% on the basis of an experiment using monochromatic light (520 nm, 26.4 mW cm^{−2}) (see the Supporting Information). The possibility of the thermodynamic reaction of **1a** to give **1a'** was investigated in water under reflux for 2 h, but no reaction

Received: March 25, 2011

Published: May 19, 2011

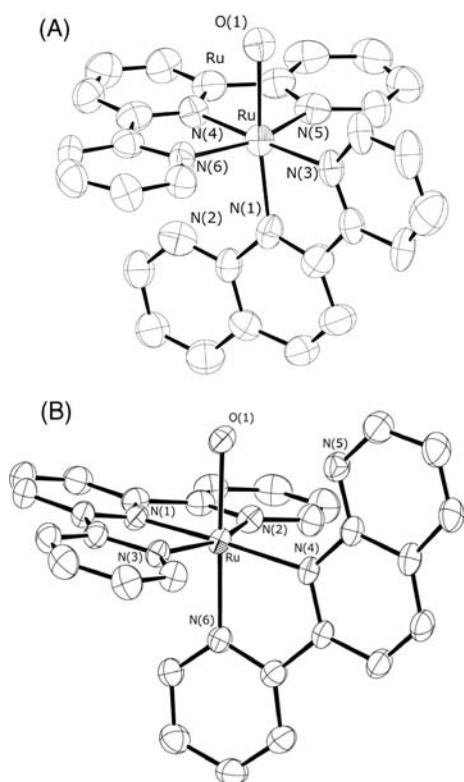
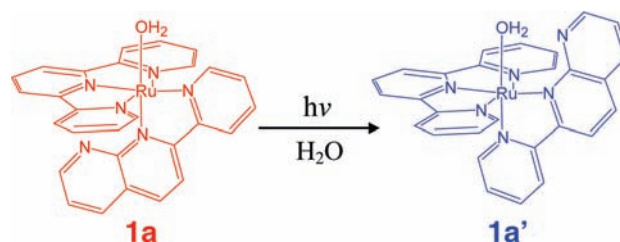


Figure 1. ORTEP plots of (A) **1a** and (B) **1a'** with 50% thermal ellipsoids.

occurred under the conditions. Although the photochemical reaction of **1a** was examined at 5–75 °C, we did not find any evidence of a photostationary state between **1a** and **1a'**.

The kinetic profile of the photoisomerization reaction was first-order with respect to **1a**. The photoisomerization rate constant (k) increased linearly with the light intensity under the conditions below 255 mW cm⁻² (Figure S6), indicating that a photoexcited state is involved in the photoisomerization under the conditions employed. The k value was constant over the pH 1–7 range but decreased drastically for pH > 7. For pH > 11, the photoisomerization did not occur at all (Figure S7). The UV–vis absorption spectral change of the **1a** solution in the pH titration gave $pK_a = 9.7$ for deprotonation of an aquo ligand of **1a** to form the hydroxo complex *trans*-[Ru(tpy)(pynp)OH]⁺ (Figure S8). The pH dependence of k corresponded to the distributed fraction of **1a** (aquo form) as a function of pH (Figure S7). This result suggests that deprotonation of the aquo ligand of **1a** makes **1a** inert toward the photoisomerization. The photoisomerization was significantly temperature-controlled, with an activation energy of 41.7 kJ mol⁻¹ at pH 5.6 (Figure S9). A possible mechanism for the photoisomerization was hypothesized on the basis of previous reports on photosubstitution reactions.^{4–6} Subsequent to generation of the ³MLCT state by visible-light excitation of **1a**, the photodissociation of an aquo ligand from **1a** could occur via the thermally accessible ³d–d state, forming a five-coordinate [Ru(tpy)(pynp)]²⁺ intermediate. The **1a'** isomer would then be produced by recoordination of a water molecule to the intermediate from the opposite side with respect to the tpy plane. There are two possible explanations for the activation process: (1) thermal activation from the ³MLCT state to the ³d–d state and (2) activation of the Ru–O bond involved in

Scheme 1. Photoisomerization of **1a** to **1a'**



dissociation of the aquo ligand. However, the first possibility cannot explain the observation that **1a'** does not undergo the reverse isomerization to **1a**, though the UV–vis spectrum of **1a'** is very similar to that of **1a** (Figure S10). The activation of the Ru–O bond could be involved in the activation process. The activation energy (41.7 kJ mol⁻¹) is consistent with the activation enthalpy (50.6–87.8 kJ mol⁻¹) for water exchange in ruthenium aquo complexes.^{25–27} The inert photoisomerization of the hydroxo complex could be explained mainly by the higher dissociation energy of the hydroxo ligand from a Ru center relative to that of the aquo ligand. However, we do not exclude the possibility of increased thermal activation to the ³d–d state from the ³MLCT state in this stage.

ORTEP plots of **1a** and **1a'** are shown in Figure 1, and the X-ray crystallographic data are shown in Tables S1–S3. In both **1a** and **1a'**, the central Ru–N_{tpy} bond [1.975(9) and 1.970(4) Å, respectively] is shorter than the other two Ru–N_{tpy} bonds [2.070(4)–2.087(8) Å], similar to the case for **1**.²⁴ In **1a**, the Ru–N bonds to the naphthyridine (np) and pyridine (py) moieties of pynp are nearly the same length [2.059(8) and 2.062(9) Å], but in **1a'**, the Ru–N_{np} bond [2.109(3) Å] is significantly longer than the Ru–N_{py} bond [2.027(4) Å]. The different Ru–N bond lengths could be caused by the steric hindrance between the aquo ligand and the bulky np moiety. The Ru–O bond [2.199(7) Å] to the aquo ligand in **1a** is 0.078 Å longer than that in **1a'** [2.121(3) Å]. The distance between the O atom of the aquo ligand and the N atom at the 8-position of np is 2.659 Å, which is consistent with the O···N distance for an O–H···N hydrogen bond.

The cyclic voltammogram (CV) of **1a** in an aqueous solution at pH 6.4 exhibited two redox waves at 0.46 and 0.63 V assigned to Ru^{II/III} and Ru^{III/IV}, respectively, over the potential range from 0 to 1.0 V, whereas after visible-light irradiation for 1 h, the corresponding CV gave only a redox wave at 0.59 V under the same conditions (pH 6.4, 0–1.0 V) (Figure S11). The half-wave potential ($E_{1/2}$) values for the Ru^{II/III} and Ru^{III/IV} couples for **1a** were discrete, and both of them were pH-dependent over the wide pH range of 1.5–10, indicating that the two-step reaction involving the separate proton-coupled one-electron reactions of the Ru^{II}–OH₂/Ru^{III}–OH and Ru^{III}–OH/Ru^{IV}=O redox couples occurs (see the Pourbaix diagrams in Figure 2). The $E_{1/2}$ value for the single redox response for **1a'** was also pH-dependent over a similar pH range, but the Pourbaix diagram of **1a'** suggests a one-step reaction involving the two-proton-coupled two-electron reaction of the Ru^{II}–OH₂/Ru^{IV}=O redox couple, in contrast to the two-step redox reaction for **1a**. This result demonstrates that the redox properties of the Ru^{II/III} and Ru^{III/IV} couples are dramatically changed by the photoisomerization of **1a** to **1a'**. It should be also noted on the diagrams that the pK_a value of the aquo ligand increased from 9.7 to 10.7 as a

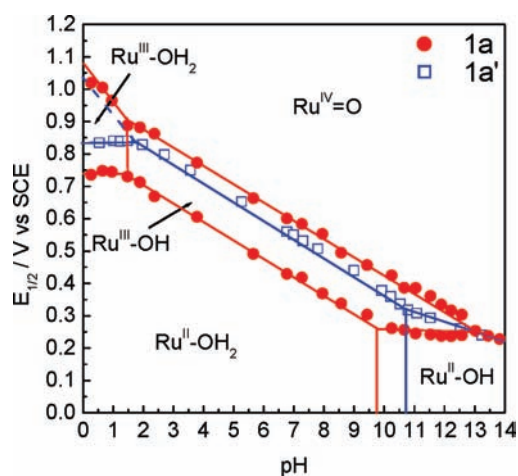


Figure 2. Pourbaix diagrams for **1a** and **1a'** in aqueous solution.

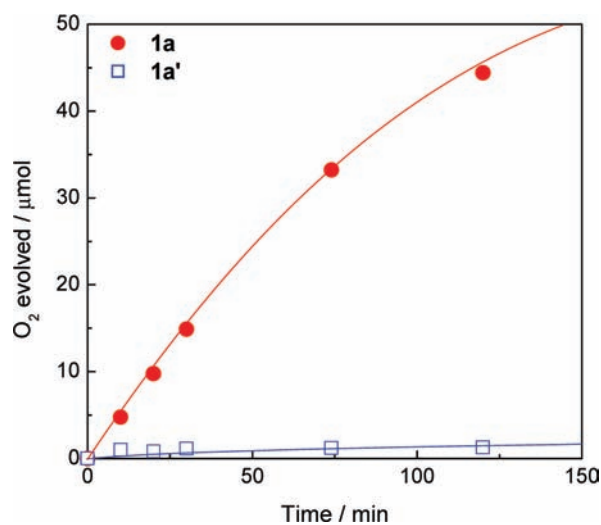


Figure 3. Time courses of the amount of O_2 evolved by **1a** (●) and **1a'** (□) in chemical water oxidation experiments in an aqueous solution at 25 °C using a Ce^{IV} oxidant. Conditions: Ce^{IV} , 0.1 M (0.5 mmol); Ru complex, 1.0 μmol ; pH 1.0; liquid volume, 5.0 mL.

result of photoisomerization of **1a** to **1a'**. This could be caused mainly by the interaction of the aquo ligand with the pynp ligand through hydrogen bonding.

In order to reveal the catalytic activities of **1a** and **1a'**, chemical water oxidation experiments were conducted in a homogeneous aqueous solution using a Ce^{IV} oxidant. O_2 was significantly evolved from the solution containing **1a** and Ce^{IV} (1.0 μmol of **1a**, 0.5 mmol of Ce^{IV} , 5.0 mL of water, pH 1.0) (Figure 3). The amount of O_2 evolved (n_{O_2}) increased with time, showing that **1a** is active for water oxidation catalysis. The initial O_2 evolution rate (ν_{O_2} in mol s^{-1}) calculated from the initial slope increased linearly with the amount of Ru (n_{Ru}). This suggests that the O_2 evolution is a first-order process with respect to **1a**. The slope of the ν_{O_2} versus n_{Ru} plot provided a turnover frequency (k_{O_2}) of $3.8 \times 10^{-3} \text{ s}^{-1}$ (Figure S12). The k_{O_2} value is slightly higher than the value of $3.4 \times 10^{-3} \text{ s}^{-1}$ for $[\text{Ru}(\text{tpy})(\text{bpy})\text{OH}_2]^{2+}$ under the same conditions. The same chemical water oxidation experiments were conducted after visible-light irradiation of the **1a** solution for 1 h to generate **1a'** completely, and n_{O_2} was found to

decrease significantly in comparison with the catalysis before the irradiation (Figure 3). The linear plot of ν_{O_2} versus n_{Ru} provided a k_{O_2} value of $4.8 \times 10^{-4} \text{ s}^{-1}$ for **1a'**, showing that k_{O_2} was decreased by nearly an order of magnitude through photoisomerization of **1a** to **1a'**. We are undertaking an advanced project to reveal the mechanism of the photoisomerization, especially the effect of hydrogen bonding between the aquo ligand and the pynp ligand on the photoisomerization, by synthesizing ruthenium(II) aquo complex derivatives with 2-(2-pyridyl)-quinoline instead of the pynp ligand.

■ ASSOCIATED CONTENT

Supporting Information. Synthesis and characterization of ruthenium complexes, experimental details, X-ray crystallographic data (CIF), substitution and photoisomerization reactions, kinetic analysis of photoisomerization, electrochemical data, and chemical water oxidation rate data. This material is available free of charge via the Internet at <http://pubs.acs.org>.

■ AUTHOR INFORMATION

Corresponding Author

yagi@eng.niigata-u.ac.jp

■ ACKNOWLEDGMENT

This research was supported by the PRESTO Program of JST and a Grant-in-Aid for Scientific Research (C) from the Ministry of Education, Culture, Sports, Science, and Technology (205-50058). We thank Prof. S. Igarashi for help with X-ray crystallographic analysis.

■ REFERENCES

- (1) Kalyanasundaram, K. *Coord. Chem. Rev.* **1982**, *46*, 159–244.
- (2) Balzani, V.; Juris, A. *Coord. Chem. Rev.* **2001**, *211*, 97–115.
- (3) Juris, A.; Balzani, V.; Barigelletti, F.; Campagna, S.; Belser, P.; Vonzelewsky, A. *Coord. Chem. Rev.* **1988**, *84*, 85–277.
- (4) Pinnick, D. V.; Durham, B. *Inorg. Chem.* **1984**, *23*, 1440–1445.
- (5) Durham, B.; Walsh, J. L.; Carter, C. L.; Meyer, T. J. *Inorg. Chem.* **1980**, *19*, 860–865.
- (6) Hecker, C. R.; Fanwick, P. E.; McMillin, D. R. *Inorg. Chem.* **1991**, *30*, 659–666.
- (7) Porter, G. B.; Sparks, R. H. *J. Photochem.* **1980**, *13*, 123–131.
- (8) Vanhouten, J.; Watts, R. J. *Inorg. Chem.* **1978**, *17*, 3381–3385.
- (9) Durham, B.; Caspar, J. V.; Nagle, J. K.; Meyer, T. J. *J. Am. Chem. Soc.* **1982**, *104*, 4803–4810.
- (10) Durham, B.; Wilson, S. R.; Hodgson, D. J.; Meyer, T. J. *J. Am. Chem. Soc.* **1980**, *102*, 600–607.
- (11) Huynh, M. H. V.; Meyer, T. J. *Chem. Rev.* **2007**, *107*, 5004–5064.
- (12) Stultz, L. K.; Binstead, R. A.; Reynolds, M. S.; Meyer, T. J. *J. Am. Chem. Soc.* **1995**, *117*, 2520–2532.
- (13) Fung, W. H.; Yu, W. Y.; Che, C. M. *J. Org. Chem.* **1998**, *63*, 7715–7726.
- (14) Masllorens, E.; Rodriguez, M.; Romero, I.; Roglans, A.; Parella, T.; Benet-Buchholz, J.; Poyatos, M.; Llobet, A. *J. Am. Chem. Soc.* **2006**, *128*, 5306–5307.
- (15) Doveloglou, A.; Adeyemi, S. A.; Meyer, T. J. *Inorg. Chem.* **1996**, *35*, 4120–4127.
- (16) Concepcion, J. J.; Jurss, J. W.; Templeton, J. L.; Meyer, T. J. *J. Am. Chem. Soc.* **2008**, *130*, 16462–16463.
- (17) Yagi, M.; Syouji, A.; Yamada, S.; Komi, M.; Yamazaki, H.; Tajima, S. *Photochem. Photobiol. Sci.* **2009**, *8*, 139–147.

- (18) Pramanik, N. C.; Bhattacharya, S. *Transition Met. Chem.* **1997**, *22*, 524–526.
- (19) Yagi, M.; Tajima, S.; Komi, M.; Yamazaki, H. *Dalton Trans.* **2011**, *40*, 3802–3804.
- (20) Wasylenko, D. J.; Ganesamoorthy, C.; Koivisto, B. D.; Henderson, M. A.; Berlinguette, C. P. *Inorg. Chem.* **2010**, *49*, 2202–2209.
- (21) Masaoka, S.; Sakai, K. *Chem. Lett.* **2009**, *38*, 182–183.
- (22) Concepcion, J. J.; Jurss, J. W.; Norris, M. R.; Chen, Z. F.; Templeton, J. L.; Meyer, T. J. *Inorg. Chem.* **2010**, *49*, 1277–1279.
- (23) Concepcion, J. J.; Tsai, M.-K.; Muckerman, J. T.; Meyer, T. J. *J. Am. Chem. Soc.* **2010**, *132*, 1545–1557.
- (24) Tseng, H. W.; Zong, R.; Muckerman, J. T.; Thummel, R. *Inorg. Chem.* **2008**, *47*, 11763–11773.
- (25) Alezra, V.; Bernardinelli, G.; Corminboeuf, C.; Frey, U.; Kündig, E. P.; Merbach, A. E.; Saudan, C. M.; Viton, F.; Weber, J. *J. Am. Chem. Soc.* **2004**, *126*, 4843–4853.
- (26) Rapaport, I.; Helm, L.; Merbach, A. E.; Bernhard, P.; Ludi, A. *Inorg. Chem.* **1988**, *27*, 873–879.
- (27) Stebler-Roethlisberger, M.; Hummel, W.; Pittet, P. A.; Büergi, H. B.; Ludi, A.; Merbach, A. E. *Inorg. Chem.* **1988**, *27*, 1358–1363.